Thermochimica Acta, 231 (1994) 239–256
Elsevier Science B.V., Amsterdam
SSDI 0040-6031(93)01194-8

Thermal transitions in surfactant-based lyotropic liquid crystals

P.C. Schulz [a,1], J.E. Puig [a,*], G. Barreiro [b] and L.A. Torres [b]

[a] *Facultad de Ciencias Químicas, Universidad de Guadalajara, Boul M. García Barragán #1451, Guadalajara, JAL. 44430 (Mexico)*
[b] *Departamento de Química, Centro de Investigación y Estudios Avanzados, Apdo. Postal 14-740, Mexico D.F. 07000 (Mexico)*

(Received 16 March 1993; accepted 2 April 1993)

Abstract

The state of water and several thermal transitions were examined in several surfactant/water lyotropic liquid crystalline systems. The surfactants studied were Aerosol OT (AOT), didodecyldimethylammonium bromide (DDAB), dioctadecyldimethylammonium bromide (DODAB) and *n*-decylphosphonic acid (DPA). In the AOT/water system, three types of water were detected: "bulk-like" water, interfacial water and hydration water (about six molecules of water per molecule of AOT). This system does not exhibit the gel–liquid-crystal transition, probably because the branched, short tails of AOT do not allow for crystallization upon cooling because of steric hindrance. In the DDAB/water and DODAB/water systems, only bulk-like water and two molecules of hydration water per molecule of surfactant were observed. The gel–liquid-crystal transition was detected at 15°C for DDAB and at 50°C for DODAB. In the DPA/water system, only bulk-like water was seen. The gel–liquid-crystal transition for this surfactant was detected at about 12°C.

INTRODUCTION

Surfactants frequently form lyotropic liquid crystalline phases by incorporating water and/or organic solvents into their structures [1,2]. Many surfactants can also yield thermotropic liquid crystals [3]. Surfactant-based liquid crystals appear in many processes and applications and they have been used as model systems for biological membranes [4–9].

Several types of water have been detected in surfactant-based liquid crystalline phases [10–13]. These "types of water" have different enthalpies and temperatures of melting, as well as anomalously low supercooling temperatures [12]. The supercooling and freezing behavior of water in non-bulk states is important in understanding the behavior of water in

* Corresponding author.
[1] Present address: Departamento de Química, Universidad Nacional del Sur, Bahía Blanca, Argentina.

microporous materials, gels, foods, biological tissues, and other microstructured fluids at sub-zero temperatures. Also, water exists in various states with different properties in living organisms. Hence, it is important to understand the nature of the different types of water in liquid crystalline systems as well as other thermal transitions such as the so-called "gel–liquid-crystal transition" [14]. Here we report vapor pressure and differential scanning calorimetry (DSC) measurements in several surfactant/water systems that form lyotropic liquid crystalline phases. The surfactants were Aerosol OT (or AOT), didodecyldimethylammonium bromide (DDAB), dioctadecyldimethylammonium bromide (DODAB) and *n*-decylphosphonic acid (DPA).

AOT is a pure double-tailed anionic surfactant that forms a lamellar phase with water from 17.5 to 75 wt.% AOT; above this concentration, it yields viscous isotropic and hexagonal phases [15–17]. DDAB is a pure double-tailed cationic surfactant that forms two lamellar phases with water that coexist at room temperature [18]. The lower-surfactant content lamellar phase (Lam_1), extending from 4 to 30 wt.% DDAB, is birefringent and has the typical mosaic texture of a lamellar phase. The other lamellar phase (Lam_2) is also birefringent but exhibits a finer mosaic texture under a polarizing microscope. This mesophase forms between 83.8 and 90 wt.% DDAB. DODAB is also a double-tailed cationic surfactant; its phase diagram with water has not been reported. However, observations with a polarizing microscope confirm that DODAB yields lamellar phases with water at room temperature. DPA is a single-tailed non-ionic surfactant that forms a lamellar phase with water at lower concentrations, and a hexagonal phase at approx. 95 wt.% [19].

EXPERIMENTAL

Sodium bis-(2-ethylhexyl)sulfosuccinate (AOT) with a purity greater than 98% was obtained from Fluka. It was dried in a vacuum oven for 24 h at 40°C and used without further purification because its purification [20] did not change its surface tension and its solubility in water, nor its phase behavior with water and tetrahydrofurfuryl methacrylate [12, 21]. Both DDAB and DODAB (Kodak), with purities greater than 99%, were recrystallized first from an acetone–ethyl ether mixture (50:50 by volume), and then from ethyl acetate and dried in a vacuum oven. DPA was synthesized and purified as described elsewhere [22]. Water was doubly distilled and deionized.

AOT samples were prepared either by direct addition of water to dried AOT, and then homogenized and allowed to equilibrate for at least 7 days at 25 ± 0.1°C, or by vapor sorption. In the latter method, dried surfactant was weighed in DSC sample pans and allowed to reach equilibrium with a large volume of NaCl aqueous solution of known water activity in a closed thermostated jar (25 ± 0.05°C). With DDAB, DODAB, and DPA, samples

were prepared by weighing surfactant and water in glass ampules that were sealed with a torch. The sealed ampules were heated to 80°C for about 24 h with continuous agitation to assure homogenization; they were then allowed to rest for one week at 25 ± 0.1°C with frequent agitation by hand.

Thermograms were obtained with a Perkin-Elmer DSC-4 calorimeter. The instrument was calibrated with indium, water and *n*-octane standards. Cooling scans below room temperature were achieved with an Intracooler I refrigeration unit (Perkin-Elmer) or with liquid nitrogen. All thermograms were determined with heating and cooling rates of 10°C min^{-1}. Aluminum samples pans for volatile samples (Perkin-Elmer) were used to minimize losses by evaporation. Samples were weighed before and after DSC runs. Results with samples that lost weight were discarded. Transition temperatures were determined (±0.5°C) upon heating from the point at which the baseline changed slope significantly. Samples were normally cooled to temperatures of −60°C or lower to ensure they were completely frozen.

Vapor pressure measurements were made in a static system with an MKS Baratron 77 pressure meter (A) with reference (Pr) and measurement (Px) chambers (Fig. 1). The 50 cm^3 glass sample cell (B) was made with a glass–metal joint. The vacuum line was made of 1/4-in nominal diameter and 4-mm inner diameter 316 ASTM stainless steel tubing and Swagelok connections. All valves (C–G) were Nupro bellows-type (SS-4BK-1C) pneumatically activated. Vacuum was achieved with a Baltzer PVA-063H diffusion pump aided with a cryogenic pump packed with 5X molecular sieve (H). Temperature was controlled within 0.005°C with an LKB 7600-A temperature bath and an LKB-7602 proportional controller. Temperature was measured with a calibrated Guildline 9535/010203 platinum resistance

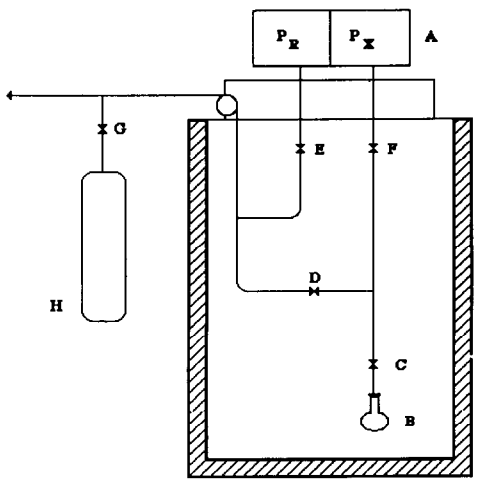

Fig. 1. Schematic of the static system for measuring vapor pressures: (A) capacitance manometer, (B) sublimation cell, (C)–(G) pneumatic bellows valves, and (H) vacuum pump.

digital thermometer. Samples were centrifuged for about 1 h and placed in the sample cell where they were degassed by freeze-pump-and-thaw cycles (usually 2 or 3 cycles were enough). Next, samples were thermally equilibrated in the cell for at least 1 h before starting the measurements. The vapor pressures reported here are the averages of at least five measurements.

RESULTS AND DISCUSSION

AOT–water system

State of water

AOT forms lamellar liquid crystals in water at concentrations between approx. 17.5 and 75 wt.% [15–17]. Figure 2 shows typical DSC thermograms of the AOT/water lamellar phase, where three thermal transitions are observed at 0, −5 and −9°C (peaks 1, 2 and 3, respectively). No other transitions are detected between −150 and 60°C. These three transitions were detected for samples with AOT concentrations of up to about

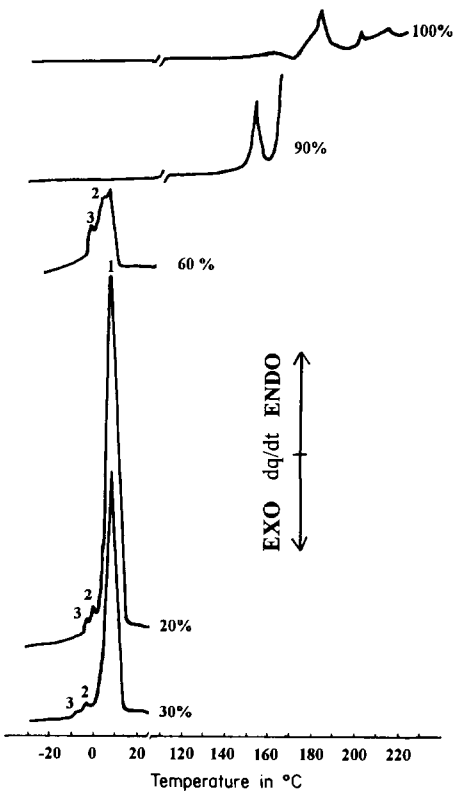

Fig. 2. DSC thermograms of AOT/water samples as a function of AOT concentration.

60 wt.%. Moreover, the area of peak 1 decreases with respect to those of peaks 2 and 3 as the concentration of AOT increases, i.e. as the water layer thickness in the lamellar phase decreases [16]. Samples with less than 70 wt.% AOT were not examined above 60°C because their thermograms were not reproducible, probably because of changes in composition.

The nature of these transitions was elucidated by comparing our results with those of AOT/D_2O samples reported elsewhere [10, 12]. All three transitions shifted by 4°C, and because the melting temperature of pure D_2O is 4°C higher than that of pure H_2O [23], it is clear that the three thermal transitions are caused by the melting of the water in the bilayers. Because there is not a separate water phase in these one-phase samples, the large peak at 0°C must be due to melting of "bulk-like" water located in thin films (<100 Å) between the bilayers of the lamellar liquid crystals. The other two peaks must be related to the melting of "interfacial" or bound water associated with the polar groups and the counterions in the bilayers.

Above 60 and up to 75 wt.% AOT, only peaks 2 and 3 are observed (Fig. 2). These results are consistent with vapor pressure measurements (Fig. 3). Below around 30 wt.% AOT, the vapor pressure of water in the lamellar phase is the same as that of pure water (23.8 mm Hg at 25°C) and remains, within experimental errror, close to this value up to about 60 wt.% AOT. At this concentration, the activity of water, determined by isopiestic vapor pressure measurements, is close to 0.99. Hence, DSC and vapor pressure

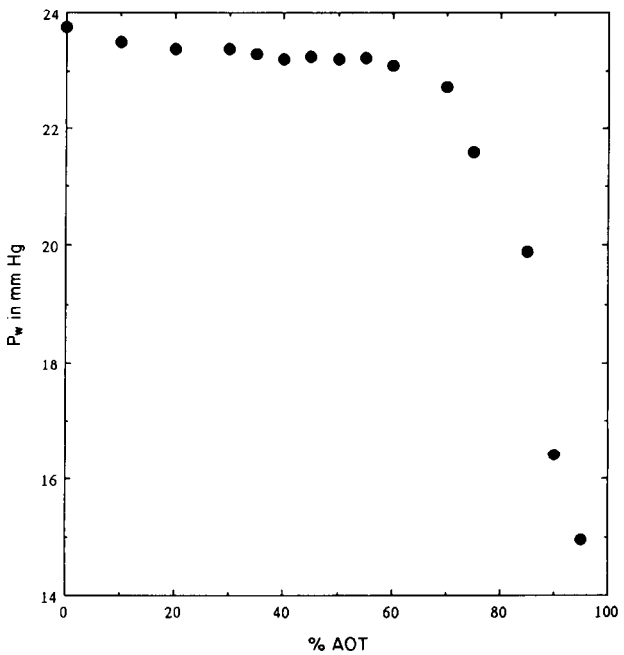

Fig. 3. Water vapor pressure in AOT/water samples as a function of AOT concentration.

TABLE 1

Melting and supercooling temperatures of water in AOT/water liquid crystalline phases

Wt.% AOT	T_{melt}/°C	$T_{freezing}$/°C
0	0	−18
10	0	−18
20	0, −5, −8	−18
30	0, −5, −8	−16
40	0, −5, −8	−16
50	0, −5, −8	−16
60	0, −5, −8	−16
61	−5, −8	−43
71	−8	−60

measurements confirm the existence of bulk-like water in lamellar phases containing less than approx. 60 wt.% AOT. Above this concentration, however, the vapor pressure of water in the bilayers drops abruptly (Fig. 3) and the peak due to bulk-like water also disappears (Fig. 2).

Bulk-like water can be supercooled to temperatures of around from −16 to −23°C [23]. However, water in thin films or in emulsified microdroplets can be supercooled to temperatures as low as −40°C 24–26]. Table 1 reports the melting and freezing temperatures of water in the lamellar phase as a function of concentration. Here one can see that water supercools to temperatures below −40°C only in those samples where there is no bulk-like water, i.e. samples with AOT concentrations greater than 60 wt.%. These results support the conclusion that in addition to bulk-like water, water strongly bound to the surfactant polar groups and to the counterions is also present and has thermodynamic properties that are different from those of bulk (or bulk-like) water.

The enthalpy of melting of water per gram of sample (Fig. 4) drops linearly with AOT concentration from that of pure water (320 J g^{-1}) to zero at 80 wt.% AOT. At this concentration, where a hexagonal phase forms [15–17], water peaks 2 and 3 vanish and there are about 6 molecules of water per molecule of AOT. Hence, this water must be strongly bound to the sodium ion and to the AOT polar group, probably as primary hydration water; therefore, it is undetectable by DSC (Fig. 2) and has a very small vapor pressure (Fig. 3).

The hydration number of Na^+ is about 5 ± 1 molecules of water [27, 28]. Hence, there should be around 1 or 2 molecules of water hydrating the sulfosuccinate group. The charge of the polar group in AOT and in phospholipids (which exhibit the same water transitions as AOT/water lamellar liquid crystals [29]) is concentrated over the oxygen atoms exposed directly to water. Oxygen atoms (0.14 nm in radius [30, 31]) are larger than sodium ions (0.097 nm in radius [23]). However, water molecules interact

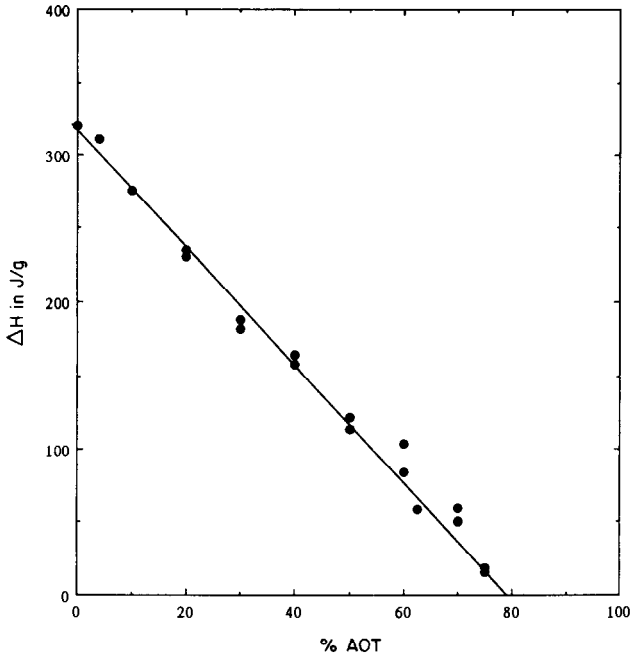

Fig. 4. Melting enthalpy of water per gram of sample as a function of AOT concentration.

more strongly with anions than with cations of the same size because the center of their positive charge can come closer to an anion than the center of their negative charge can approach a cation [32, 33]. As a result, phosphonate groups, which are similar to the phosphate groups of phospholipids, have hydration numbers of around 1.5 [34]. Hence, in the AOT/water system there must be 6–8 molecules of hydration water. Of these, 5 ± 1 are strongly bound to the sodium ion and the rest (1 or 2) are bound to the surfactant polar group.

In summary, DSC and vapor pressure measurements have demonstrated that there are three types of water in lamellar liquid crystals of AOT/water.

(i) "Bulk-like" water or water 1. This type of water is located in the bilayers but it does not interact with the polar groups and the counterions, and behaves like bulk water.

(ii) "Interfacial" water or water 2 and 3 (about 10 molecules of water per molecule of AOT). This type of water is much more weakly bound to the ionic groups than the molecules of primary hydration water, and its participation in the hydrogen bonding structure of water is weaker than that of water 1. As a consequence, interfacial water "melts" at lower temperatures than bulk water, so its vapor pressure must be smaller than that of bulk water. In fact, the vapor pressure of water in a 30 wt.% AOT sample at −4°C is 3.38 mm Hg, as compared to 3.41 mm Hg for bulk water at the same temperature.

(iii) Primary hydration water. This type of water (about 6 molecules of water per molecule of AOT) is strongly bound to the counterions and the polar groups, and is undetectable by DSC.

The gel–liquid-crystal transition and other transitions

Many surfactant/water lamellar liquid crystals exhibit the gel–liquid-crystal transition [14]. This transition corresponds to the "melting" of the hydrocarbon tails of the surfactant in the bilayers from an ordered trans configuration at lower temperatures to a more disordered fluid state at higher temperatures. This melting is accompanied by a lateral expansion and a decrease in the thickness of the bilayers [14].

The lack of thermal transitions other than the water transitions between −150 and 100°C, is significant and indicates that there is no gel–liquid-crystal transition in the AOT/water system. The melting points of *n*-octane and its isomers range from about −57 to −110°C [23]. Hence, if a gel–liquid-crystal transition were to exist in the AOT/water lamellar mesophase, it should occur at temperatures well below 0°C. However, no such transition is detected by DSC in the temperature range examined. The reason is probably steric, i.e. the short and branched tails of AOT may not be able to pack in the frozen state to form a solid crystalline structure; instead, they must form an amorphous state upon cooling and hence they must have a very small enthalpy of melting. Amphiphiles with branched and short tails or unsaturated tails usually crystallize with difficulty or not at all. Using adiabatic calorimetry, Czarniecki et al. [10] reported a "broad pretransitional region" in the AOT/D_2O lamellar phase starting at −50°C. This transition may be due to the gradual (non-abrupt) chain melting of AOT.

Above 80 wt.% AOT, a sharp transition is detected between 140 and 150°C which is probably associated with a liquid crystal–isotropic phase transition (Fig. 2). This peak is not detected if the sample is heated above 160°C, then cooled down to 25°C and reheated, but it is observed again with a fresh sample. In temperature cycles above 160°C, the transition is not detected, probably because of a hydrolytic decomposition of the sample.

Pure AOT is a waxy, very hygroscopic solid. X-ray diffraction studies indicate that pure AOT is a hexagonal liquid crystal at room temperature [16]. AOT forms a fluid-like isotropic phase at 160°C [15, 16], in agreement with our DSC results (Fig. 2). Above 180°C, pure AOT decomposes.

DDAB/water and DODAB/water systems

State of water

Thermograms of DDAB/water systems upon heating are shown in Fig. 5A. As reported elsewhere [18], DDAB/water forms two types of lamellar

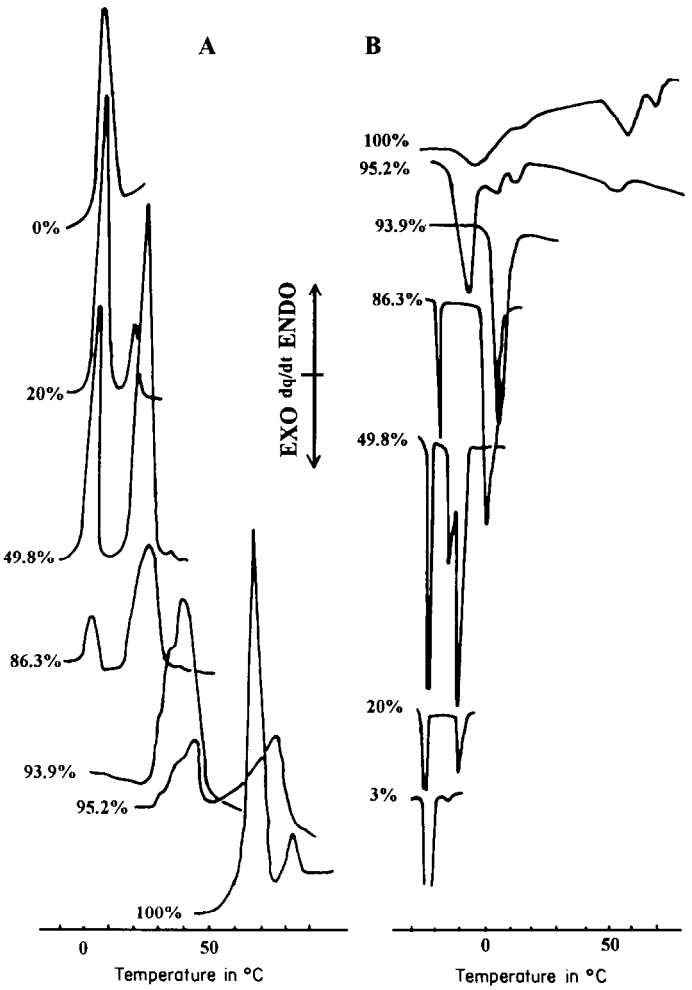

Fig. 5. DSC thermograms of DDAB/water samples as a function of DDAB concentration upon heating (A) and upon cooling (B).

phases: one between 4 wt.% and 30 wt.% DDAB, and the other between 83 wt.% and 90 wt.% DDAB. Up to DDAB concentrations of around 93 wt.%, only two peaks are detected, one at 0°C and the other at about 15°C (which corresponds to the melting of the surfactant tails as we discuss below); the latter transition shifts slightly with DDAB concentration. To demonstrate the peak at 0°C corresponds to melting of bulk-like water in the bilayers, DSC measurements on a 10 wt.% DDAB/D_2O sample (not shown) were performed. The texture of this sample, the myelins structures and maltese crosses observed with a polarizing microscope, is identical to that of a sample of identical composition but made with H_2O. Again, only two transitions are observed between −150 and 80°C: one at 4°C and the other at 15°C. Because D_2O melts 4°C higher than water [23], it is clear that

the transition detected at the lower temperature is due to bulk-like water, inasmuch as no separate water phase is present in samples with concentrations higher than 4 wt.% DDAB [18]. The water peak remains at 0°C in heating scans up to about 93 wt.% DDAB, after which the water peak is no longer detected. Upon cooling, the water transition is detected at about −16°C, shifting to about −23°C at around 90 wt.% DDAB (Fig. 5B). These values are within the normal range of supercooling temperatures of bulk water [23]. Also, the vapor pressure of water in these samples is high and similar to that of bulk water up to concentrations of around 90 wt.% DDAB (Fig. 6), supporting our conclusion that "bulk-like" water is present in this system up to high DDAB concentrations.

The enthalpy of melting of water per gram of sample is shown in Fig. 7 (curve I). Here it can be seen that the enthalpy of water decreases monotonically with DDAB concentration and becomes zero at about 93 wt.% DDAB. At this concentration there are 2 molecules of water per molecule of DDAB. Notice that upon heating (Fig. 5A) or cooling (Fig. 5B) a 93.92 wt.% DDAB sample, the water peak is no longer detected. Hence, the conclusion is that in DDAB/water lamellar phases, independent of the

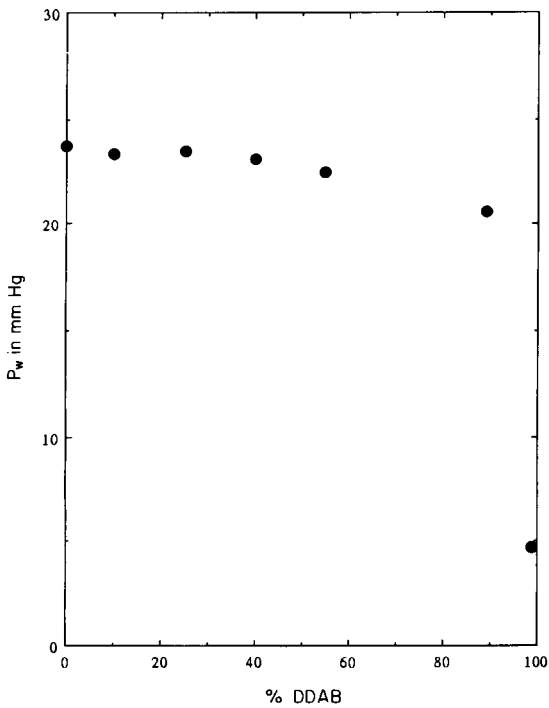

Fig. 6. Water vapor pressure in DDAB/water samples as a function of DDAB concentration.

type of lamellar phase, water behaves as "bulk-like" water located in the bilayers of the lamellae, with the exception of two molecules of water per molecule of DDAB.

The charge in the tetraalkylammonium ion is located on the nitrogen atom which is surrounded by hydrophobic alkyl groups. In addition, this ionic group is large and has a low surface charge density. Consequently, it must have a negligible primary hydration capacity [35, 36]. The bromide ion, also being large, has a hydration number of about 2 [23]. Hence, the two hydration water molecules must be mainly bound to the bromide ion.

Similar conclusions can be drawn for the DODAB/water system. The phase diagram of DODAB/water has not been reported. However, DODAB/water samples with low and high surfactant content exhibit birefringence and the typical mosaic texture of a lamellar phase when they are examined under a microscope with crossed polarizers. Figure 8 shows DSC thermograms of DODAB/water samples as a function of DODAB concentration. Again, only two peaks are detected up to DODAB concentrations of around 95 wt.% (Fig. 8A). One peak appears at 0°C, corresponding to the melting of bulk-like water in the bilayers. The other is

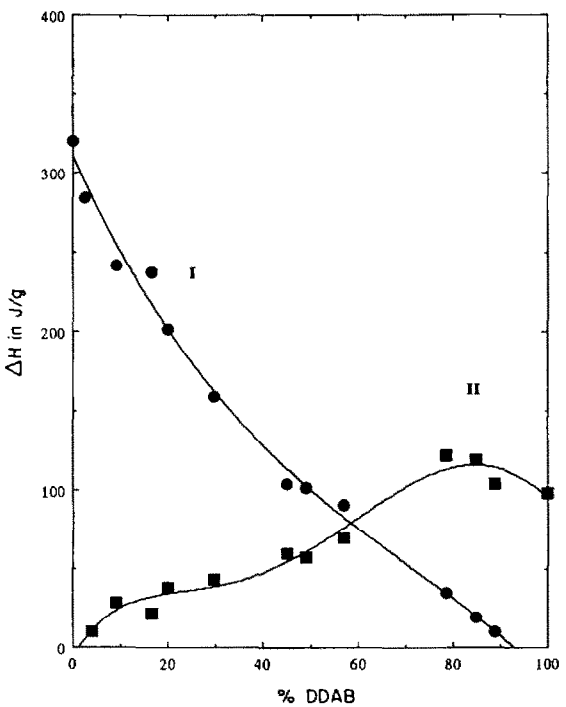

Fig. 7. Melting enthalpy of water per gram of sample (curve I) and melting enthalpy of the hydrocarbon tails per gram of sample (curve II) as a function of DDAB concentration.

detected at approx. 50°C and is due to the melting of the surfactant tails as discussed below. Upon cooling, the water peak is detected at temperatures of around −16°C (Fig. 8B) which again corresponds to typical supercooling temperatures of bulk water [23]. Figure 9 (curve I) shows that the enthalpy of melting of water per gram of sample decreases as DODAB concentration increases and becomes zero at around 97 wt.% DODAB. At this concentration, there are about 2 molecules of water per molecule of DODAB. Hence, in the DODAB/water system, as in the DDAB/water system, most of the water is located in the bilayers as "bulk-like" water and only two molecules of water per molecule of amphiphile are primarily hydrating the bromide ion.

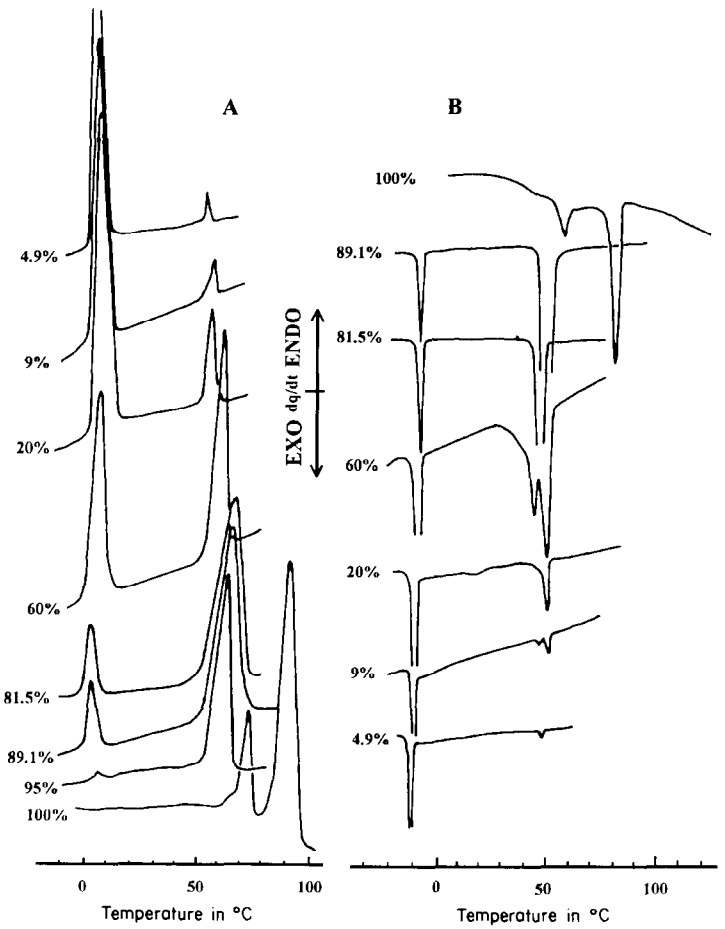

Fig. 8 DSC thermograms of DODAB/water samples as a function of DODAB concentration upon heating (A) and upon cooling (B).

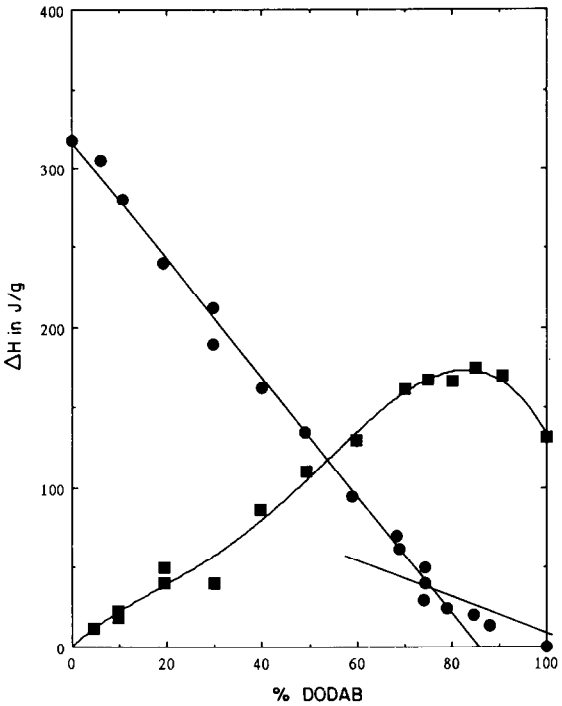

Fig. 9. Melting enthalpy of water per gram of sample (curve I) and melting enthalpy of hydrocarbon tails (curve II) per gram of sample as a function of DODAB concentration.

The gel–liquid-crystal transition and other transitions

Upon heating, the hydrocarbon tails of pure DDAB melt at about 60.7 ± 0.3°C (thermogram of 100% DDAB in Fig. 5A) with an enthalpy of 83.3 J per g of sample, or 61.0 J per g of hydrocarbon chains (Fig. 7); *n*-dodecane melts at −9.6°C with an enthalpy of melting of 214.8 J^{-1} g [23]. The smaller enthalpy of fusion of the DDAB hydrocarbons tails as compared to that of *n*-dodecane, is the result of the higher melting temperature of the DDAB hydrocarbon tails in agreement with Kirchhoff's law. The higher melting temperature of the hydrocarbon tails is caused by the additional cohesion provided by the polar groups in the crystals of DDAB. For instance, the hydrocarbon tail of sodium mystiriate melts at 113°C [37, 38], whereas *n*-tridecane melts at −5°C [23]. The higher melting temperatures of the chains of sodium mystiriate also reflect the larger cohesion and closer packing in this soap as compared to those in DDAB. This is also the reason why pure DDAB melts at a much lower temperature (76.5°C) (see thermogram for 100% DDAB in Fig. 5A) than sodium mystiriate (257°C) [37, 38]. The measured melting enthalpy of DDAB is 17 ± 1 $J g^{-1}$.

Upon addition of water, the DDAB melting transition shifts to lower temperatures, becomes broader, and vanishes when the peak due to

bulk-like water appears. The peak of the hydrocarbon tails, in turn, becomes broader upon addition of water and it shifts to lower temperatures (Fig. 5A) because the cohesion of the ionic layers becomes weaker in the presence of water. Also, several shoulders appear in the hydrocarbon-tail peak. Cooling thermograms of samples above 93.9 wt.% DDAB also show the appearance of shoulders and extra peaks (Fig. 5B). Notice that the melting temperature of the hydrocarbon chains, i.e. the gel–to–liquid-crystal transition, is invariant (approx. 15°C) once the water peak appears (see Fig. 5A).

As discussed above, at 93.9 wt.% DDAB there are two molecules of hydration water per molecule of DDAB. At this concentration, only one peak is detected (notice that the peak due to the melting of the polar group has vanished). This peak corresponds to the melting of the dihydrated compound. The formation of shoulders and the shifting of this peak at concentrations greater than 93.9 wt.% DDAB is probably due to the formation of stoichiometric compounds of dihydrated and pure DDAB. Again, in agreement with Kirchhoff's law, the enthalpy of melting of the tails increases as the melting point decreases (Fig. 7, curve II). Once the gel–liquid-crystal transition remains invariant, its enthalpy decreases linearly with DDAB concentration, as expected.

A careful examination of the peak due to the gel–liquid-crystal transition indicates that it is composed of the superposition of two peaks over the whole concentration range. Sometimes, a shoulder is seen on the main peak, but in some cases, two very close peaks can be discerned (see 49.8 wt.% DDAB sample in Fig. 5B). This result suggests that the two hydrocarbon chains are not totally equivalent. The appearance of two superimposed or separate peaks is seen in both lamellar phases in this system.

DODAB/water samples exhibit transitions similar to those of DDAB/water samples. Upon heating pure DODAB, two transitions are detected. The first at 69°C corresponds to the melting of the hydrocarbon tails and is substantially higher than that of octadecane (28°C) [23] because of the extra cohesion provided by the polar groups in the DODAB crystalline form. The other transition at 86°C is due to melting of the DODAB crystals (see thermogram of 100% DODAB in Fig. 8A). The melting temperature of DODAB is higher than that of DDAB because of the larger cohesion provided by the longer hydrocarbon tails of DODAB.

At about 96 wt.% DODAB, where the dihydrated compound forms, the DODAB crystal melting transition can no longer be detected (Fig. 8A). Also, the chain melting transition shifts to lower temperatures until the peak due to bulk-like water appears, then it remains invariant at about 50°C (Fig. 8). The enthalpy of the chain melting transition increases as the transition temperature increases but then it decreases linearly with DODAB concentration once it remains invariant (Fig. 9, curve II).

Also, and in a similar fashion to the DDAB/water system, the chain melting peak transition appears to be the superposition of two peaks (see thermogram of the 9 and 60 wt.% DODAB samples in Fig. 5B) which suggests that the two hydrocarbon tails of DODAB are also not completely equivalent.

DPA/water system

State of water

In contrast to the systems discussed previously, the peak due to melting of bulk-like water in the DPA/water systems is present over the whole concentration interval (Fig. 10). The vapor pressure (not shown) remains practically constant, with a value similar to that of pure water for concentrations well above 90 wt.% DPA. The melting enthalpy of water per gram of sample, shown in Fig. 11 (curve I), goes to zero as the

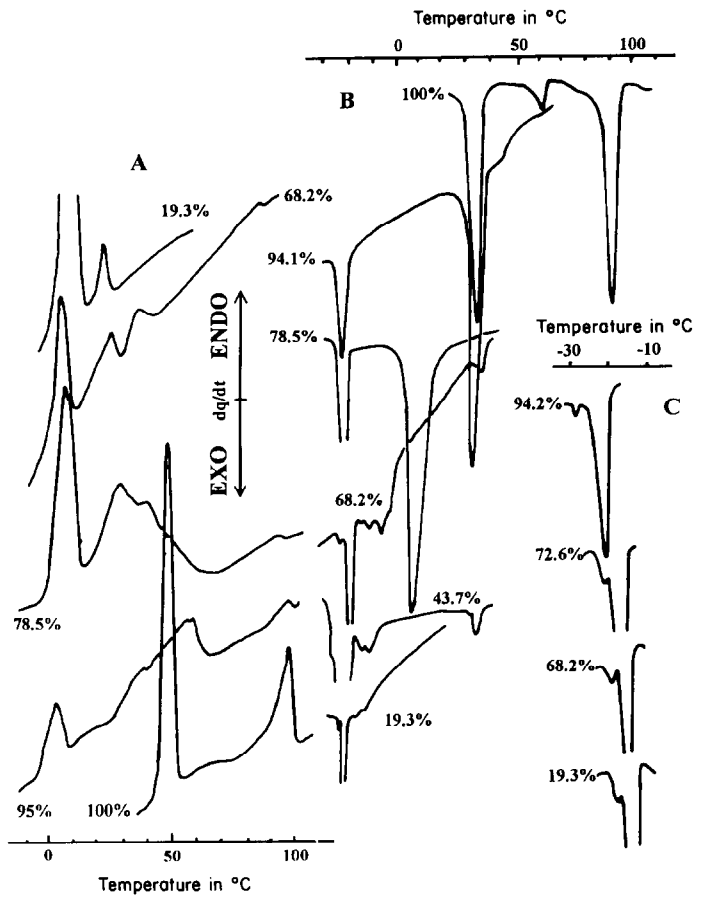

Fig. 10. DSC thermograms of DPA/water samples as a function of DDAB concentration upon heating (A) and upon cooling (B). Thermograms (C) show the water supercooling peaks in more detail.

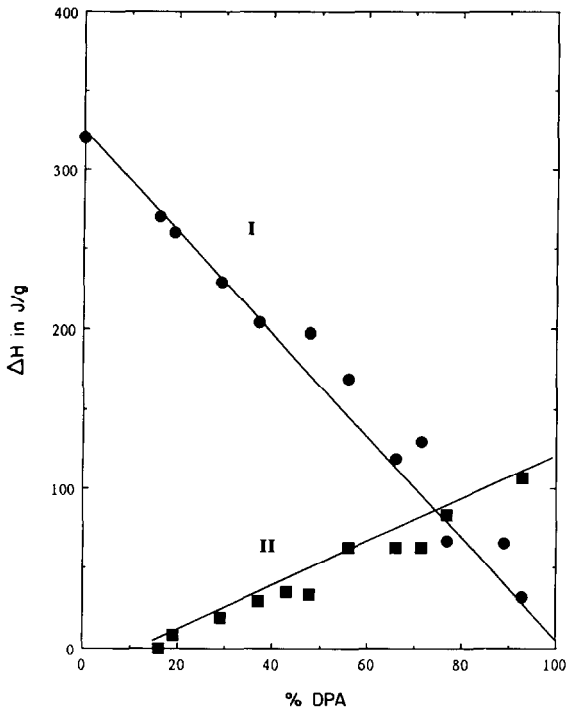

Fig. 11. Melting enthalpy of water per gram of sample (curve I) and melting enthalpy of the hydrocarbon tails per gram of sample (curve II) as a function of DPA concentration.

concentration of DPA becomes 100%. These results indicate that water behaves as "bulk-like" water and interacts very weakly with the PO_3H_2 groups in all proportions. In fact, these groups are large and weakly dissociated. Consequently, their interactions with water molecules are dipole–dipole type at relatively large distances, and no primary hydration water is bound to them.

However, upon freezing there are two peaks caused by the supercooling of water: one that appears at −16°C, which is the typical supercooling temperature of bulk-like water, whose area decreases as the concentration of DPA increases, and another at lower temperatures (−20°C) with a solidification enthalpy of 47.2 ± 3.3 J g^{-1} (Fig. 10C). The latter peak may be due to water weakly associated to the polar groups. In fact, the constancy of the solidfication enthalpy per gram of DPA supports this conclusion. However, in the light of the results presented above, it appears that the type of water–DPA association is rather weak.

Gel–liquid-crystal transition and other transitions

DPA is a crystalline solid with a triclinic arrangement, having four molecules per elementary cell [39]. When pure DPA is heated, three thermal transitions can be detected at 43.9, 52.8 and 89.2°C (see

thermogram for 100% DPA in Fig. 10). The transition occurring at 43.9°C corresponds to a change from an ordered crystalline structure to a more disordered one, in which the hydrocarbon tails are more fluid, as detected by FTIR [19], and the polar group association is slightly disrupted by a reduction in the hydrogen bonding of the $-PO_3H_2$ groups in the solid crystal. The enthalpy of this transition is $97.5 \pm 8.8\ J\ g^{-1}$. In the second transition, at 52.8°C, the structure changes visually to that of a "waxy solid", with an enthalpy of $21.3 \pm 0.2\ J\ g^{-1}$. In this structure, hydrogen bonding among polar groups is still strong. Finally, at 89.2°C, the solid structure melts completely and an isotropic fluid phase forms. The enthalpy of this transition is $59.0 \pm 3.8\ J\ g^{-1}$.

Upon addition of water, DPA forms an inverted hexagonal phase up to 95 wt.% DPA [19]. All the transitions detected with pure DPA become weaker and broader because the crystalline structure of pure DPA is disrupted upon addition of water; see the thermogram for 95% DPA in Fig. 10 and the appearance of a water peak at 0°C.

The gel–liquid-crystal transition is detected in this system at about 15°C and remains invariant from DPA concentrations of 16 wt.%, where the lamellar phase forms, up to approx. 80 wt.%. The enthalpy of the gel–liquid-crystal transition decreases with the concentration of DPA (Fig. 11, curve II). There is also another transition at about 27°C where the sample becomes a colorless gel upon cooling, and then turns into a white paste. A more detailed phase diagram of the DPA/water system as a function of temperature is published elsewhere [19].

ACKNOWLEDGMENTS

The authors acknowledge the support of CONACYT through grant PCEXNA-050720 and COSNET. P.C.S. acknowledges the support of Industrias Resistol S.A. through the Programa IRSA-Universidad.

REFERENCES

1 P. Ekwall, Adv. Liq. Cryst., 1 (1975) 1.
2 G.J.T. Tiddy, Phys. Rev., 57 (1980) 1.
3 B.-I. Tamamushi, Pure Appl. Chem., 48 (1976) 441.
4 G.H. Brown, Am. Sci., (Jan–Feb.) (1972) 64.
5 A.A. Oswald, H. Huang, J. Huang and P. Valint, Jr., US Patent 4,434,062, 1984.
6 A.M. Schwartz in R.J. Good and R.R. Stromberg (Eds.), Surface and Colloid Science, Vol. 11, Plenum Press, New York, 1984.
7 S.E. Friberg, J. Colloid Interface Sci., 37 (1971) 291.
8 S.E. Friberg, A.J. Ward, S. Gunsel and F.E. Lockwood, in G. Biresaw (Ed.), Tribology and the Liquid Crystalline State, ACS Symp. Ser., 441 (1990).
9 G.H. Brown and J.J. Wolken, Liquid Crystals and Biological Structures, Academic Press, New York, 1979.
10 K. Czarniecki, A. Jaich, J.M. Janik, M. Rachwalska, J.A. Janik, J. Krawczyk, K. Otnes, F. Volino and R. Ramasseul, J. Colloid Interface Sci., 92 (1983) 358.

11 A. Faure, J. Lovera, P. Grégoire and C. Chachaty, J. Chim. Phys., 82 (1985) 779.
12 N. Casillas, J.E. Puig, R. Olayo, T.J. Hart and E.I. Franses, J. Colloid Interface Sci., 5 (1989) 384.
13 A. Goto, H. Yoshioka, H. Kishimoto and T. Fujita, Langmuir, 8 (1992) 441.
14 J.F. Baret in C.A. Cadenhead and J.F. Danielli (Eds.), Progress in Surface and Membrane Science, Vol. 14, Academic Press, New York, 1981, p. 292, and references therein.
15 E.I. Rogers and P.A. Winsor, Nature, 216 (1967) 477.
16 K. Fontell, J. Colloid Interface Sci., 44 (1973) 318.
17 E.I. Franses and T.J. Hart, J. Colloid Interface Sci., 94 (1983) 1.
18 K. Fontell, A. Ceglie, B. Lindman and B. Ninham, Acta Chem. Scand., A40 (1986) 247.
19 P.C. Schulz, M. Abrameto, J.F.A. Soltero-Martínez, A. González-Alvarez and J.E. Puig, Phase diagrams of *n*-decane and *n*-dodecanephosphonic acids in water, Mol. Cryst. Liq. Cryst., submitted.
20 A.N. Maitra and H.-F. Eicke, J. Phys. Chem., 85 (1981) 2687.
21 A.P. Full, J.E. Puig, L.U. Gron, E. W. Kaler, J.R. Minter, T.H. Mourey and J. Texter, Marcomolecules, 25 (1992) 5157.
22 P.C. Schulz and A.L.M. Leong, Rev. Latinoamer. Quím., 7 (1976) 9.
23 R.C. Weast (Ed)., Handbook of Chemistry and Physics, 61st edn., CRC Press, Boca Raton, FL, 1980, pp. B-100, D-175, F-51.
24 F. Broto and D. Clausse, J. Phys. C, 9 (1976) 4251.
25 W. Drost-Hansen, Ind. Eng. Chem., 61 (1969) 10.
26 F.M. Etzler and T.M. Liles, Langmuir, 2 (1986) 797.
27 Th. Ackermann, Discuss. Faraday Soc., 24 (1957) 180.
28 H.S. Frank and W.Y. Wen, Discuss. Faraday Soc., 24 (157) 133.
29 L. Ter-Minassian-Saraga and G. Madelmont, J. Colloid Interface Sci., 81 (1981) 369.
30 V. Vand, A. Aitken and R.K. Campbell, Acta Crystallogr., 2 (1949) 398.
31 J.E. Spice, Enlace Químico y Estructura Molecular, Alhambra, Madrid, 1970.
32 R.M. Noyes, J. Am. Chem. Soc., 84 (1962) 513.
33 A.D. Buckingham, Discuss. Faraday Soc., 24 (1957) 151.
34 P.C. Schulz, An. Asoc. Quim. Argent., 72 (1984) 529.
35 B.E. Conway, Ann. Rev. Phys. Chem., 17 (1966) 481.
36 B.E. Conway, J.E. Desnoyers and A.C. Smith, Proc. R. Soc. London Ser. A, 256 (1964) 389.
37 R.D. Vold and M.J. Vold, J. Am. Chem. Soc., 61 (1939) 808.
38 R.D. Vold, R. Reivere and J. McBain, J. Am. Chem. Soc., 63 (1941) 1293.
39 P.C. Schulz, An. Asoc. Quim. Argent. 71 (1983) 271.